Soft x-ray resonant magnetic reflectivity study of thin films and multilayers

J. M. Tonnerre,[a] L. Sève, A. Barbara-Dechelette, F. Bartolomé, and D. Raoux
Laboratoire de Cristallographie, CNRS/Université Joseph Fourier, B.P. 166, 38042 Grenoble Cedex 9, France

V. Chakarian
Naval Research Laboratory, Code 6345, Washington, D.C. 20375

C. C. Kao
National Synchrotron Light Source, Brookhaven National Laboratory, Upton, New York 11973

H. Fischer and S. Andrieu
LPM, CNRS/Université Nancy, 54506 Vandoeuvre, France

O. Fruchart
Laboratoire Louis Néel, CNRS/Université Joseph Fourier, B.P. 166, 38042 Grenoble Cedex 9, France

Soft x-ray resonant magnetic reflectivity measurements on thin films and multilayers in a *transverse* geometry using linear polarized photons are presented. Magneto-optic calculations taking into account the layer roughness allows us to reproduce all the experimental features of the angular and energy reflectivity curves as well as the asymmetry ratio in both cases. Application to Fe_xMn_{1-x} alloy films epitaxially grown on Ir(001) brings more insights on the magnetic transition occurring at $x=0.75$. © *1998 American Institute of Physics.* [S0021-8979(98)49911-0]

Magnetism in artificially made materials has become an area of intense activity. The study of magnetism of ultrathin films and multilayers has revealed new properties which are different from bulk materials and have technological potential, especially in magnetic memories and magnetic based sensors. Since the devices to be implemented concern multilayered and multielement systems, it is necessary to go beyond the measurements of the macroscopic magnetic properties and to separate out the magnetic signatures of the different species within the different layers. In order to selectively probe the magnetic contributions, we develop the use of the x-ray resonant magnetic scattering (XRMS), especially in the soft x-ray range.

XRMS, which is x-ray magnetic dichroism in a scattering condition, presents the advantage of being atom and shell selective and then allows one to probe the magnetism of the different atomic levels of a specific element in a magnetic material.[1,2] The angular dependence inherent to a scattering measurement brings furthermore the spatial selectivity. As XRMS is a two photon process, the effects related to magnetic circular dichroism (XMCD) are observable not only with circular polarized photons but also with linear polarized ones.[3,4] Moreover, they are enhanced in diffraction conditions due to interference effects and, in that case, the magnetization dependent contribution may be of the same order of magnitude as the nonmagnetic one.[5] This has been shown by using artificial large period structures, like Ag/Ni and Ag/NiFe multilayers, in order to diffract photons of large wavelength ($\lambda \approx 15$ Å at the Ni $L_{2,3}$ edges). These first experiments, where the energy dependence of an asymmetry ratio $R=(I^+-I^-)/(I^++I^-)$ is measured, I^+ and I^- being two Bragg peak intensities collected for two opposite directions of an applied magnetic field, allowed us on one hand to demonstrate the equivalence between the XMCD and the XRMS[6] and on the other hand to determine the amplitude of the magnetic moment of both $3d$ transition metals in a binary alloy.[7] In order to study thin films, which do not give Bragg peaks at small values, we have to turn to the analysis of magnetic specular reflectivity measurements.

Following the success of XMCD measurements in the soft x-ray range, specular resonant magnetic reflectivity has been mainly measured using circular polarized incident photons in a geometry similar to the *longitudinal magneto-optic Kerr effect*.[4,8,9] In the simulations, although general trends are well understood,[4] some discrepancies still remain. One possible reason is related to the difficulty to take into account the roughness at the interfaces when both states of linear horizontal and vertical polarization of the photons are coupled and then to account for its effect on the change of the circular polarization rate at each interface. Therefore, we first focused on the development of the resonant magnetic reflectivity in the *transverse magneto-optic Kerr effect* geometry, using linear p-polarized photons. The fact that the photon beam has only one polarization state allows us to straightforwardly extend the Vidal and Vincent formalism to treat the interface roughness.[10]

The measurements were conducted at the $U4B$ beam line at the National Synchrotron Light Source. A vacuum compatible θ–2θ spectrometer, working in the horizontal plane, was used.[11] The sample was magnetized by using a Bitter electromagnet capable of delivering a field up to 1400 G perpendicular to the diffraction plane. First results were obtained from a bcc W(32 Å)/Fe(91 Å)/W(129 Å) deposited by laser ablation on a Al_2O_3 substrate. Figure 1(a) shows an angular scan where the reflected intensities and the asymmetry ratios R are collected at a selected energy in the vicinity of the L_3 Fe edge. Figure 2(a) displays an energy scan where

[a]Electronic mail: tonnerre@polycnrs-gre.fr

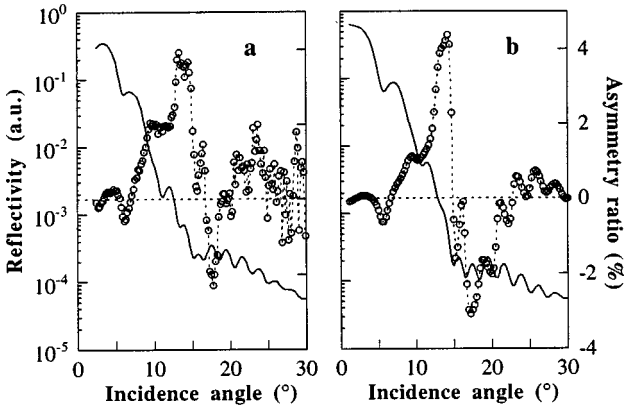

FIG. 1. Fixed energy angle scans (solid line, left side legend) and asymmetry ratio (open circles, right side legend) measured on a W/Fe/W thin film in the vicinity of Fe L_3 edge (703.2 eV): experiment (a) and calculation (b).

the angular position is kept fixed and the incident photon energy is scanned through the Fe $L_{2,3}$ edges. In this transverse geometry, the amplitude at maximum of R are typically of the order of 5% to 15% depending on both the incident angle and energy. Both scans depend on the strong resonance available at the $L_{2,3}$ edges and on the structural features of the layers: thickness and density of the layers as well as interface roughness. The energy scan is more sensitive to the spectroscopic aspect (amplitude of the magnetic moment) and the angular one to the structural aspect (arrangement of the moments).

To analyze the data, we have developed a numerical calculation based on an optical approach, where the Maxwell's equation are solved in a matrix formalism. It allows us to reproduce all the features of the experimental curve [Figs. 1(b) and 2(b)]. The main part is to calculate the dielectric tensor which has only diagonal terms in a cubic symmetry and to take into account the magnetic effects through nonvanishing off-diagonal elements. Both the imaginary and real parts of the charge dielectric constant were derived from absorption data and their Kramers–Kronig transformation, respectively. Their magnetic counterparts are determined in the

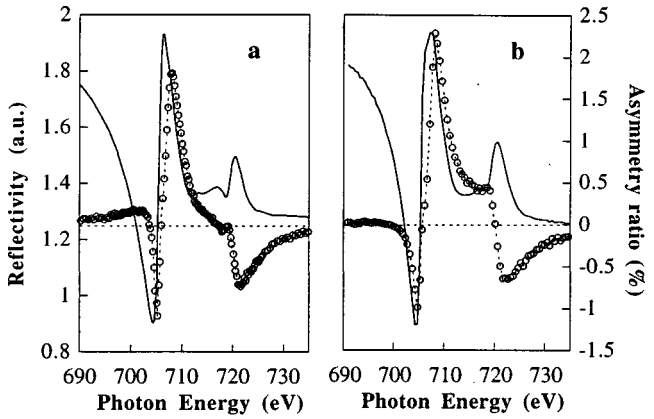

FIG. 2. Fixed angle energy scans (solid line, left side legend) and asymmetry ratio (open circles, right side legend) measured on a W/Fe/W thin film at 5° at the Fe $L_{2,3}$ edges: experiment (a) and calculation (b).

same way from XMCD data obtained from thin Fe films. That amounts to consider $M_{\mathrm{Fe}}=2.1\ \mu$B as derived from sum rules.[12] Since it is usually accepted that XMCD is proportional to the magnetic moment, we use a multiplying factor to reduce or increase the magnetic contribution to the reflectivity in order to fit our data. More details on the calculation will be given in an upcoming article.[7]

We turn next to the discussion of an example where soft x-ray resonant magnetic reflectivity has been used to investigate the magnetic transition occurring in thin $\mathrm{Fe}_x\mathrm{Mn}_{1-x}$ alloy films epitaxially grown on Ir(001). While bulk alloys present a fcc structure and are antiferromagnetic (AF) over the whole range of composition, it has been shown that, in $\mathrm{Fe}_x\mathrm{Mn}_{1-x}$/Ir superlattices (SL), the alloy is body-centered tetragonal (bct) and exhibit a magneto-structural transition at $x=0.75$ from a ferromagnetic state ($x>0.75$) to an antiferromagnetic one ($x<0.75$).[13] In the present study, we focused on two superlattices $\mathrm{Fe}_{0.9}\mathrm{Mn}_{0.1}$(27 Å)/Ir(18 Å) and $\mathrm{Fe}_{0.7}\mathrm{Mn}_{0.3}$(27 Å)/Ir(18 Å), grown on a Ir buffer layer, whose concentrations have been chosen on each sides of the transition. In the 70% Fe sample, the alloy layer is uniformly strained all through the stacking sequence of the superlattice in a bct structure with $c/a=1.23$.[14] In the 90% Fe sample, two phases have been identified.[14] In the first phase, labelled SL1, the alloy and Ir layers undergo the influence of the Ir buffer layer and the alloy layer is bct with $c/a=1.16$. In the second one, SL2, both layers have relaxed the strain imposed by the buffer layer and may be considered as free layers in mutual strain. In that case, the alloy tends to the Fe bcc structure with $c/a=1.08$. The analysis of a series of reciprocal-space maps of the diffracted intensities, collected around the (111) Bragg peak of the buffer layer for different grazing incident angles, allowed us to appreciate their proportion, which corresponds to 60% and 40%, respectively, and their localization.[15] These findings have been supported by the characterization of two thin alloy films of the same composition ($x=0.7$ and 0.9) with similar thicknesses ($\approx$30 Å) sandwiched between Ir layers, aimed at the determination of the structural properties of the alloy layers at the beginning of the elaboration process. This is of particular interest in order to separate out the magnetic properties of SL1 and SL2.

Figure 3 shows the energy dependence of R measured at 15° on both multilayers around the Fe $L_{2,3}$ edges. The shapes of R are similar and they exhibit two resonances at the L_3 (707 eV) and L_2 edge (720 eV). Fe atoms in the Fe 90% SL give rise to a strong asymmetry ratio of about 40% while for the Fe 70% SL, R values are at most 4%. This reduction of the magnetic signal of the Fe atoms is far beyond the change one would expect from its concentration reduction. The simulation of the energy dependence of R has been carried out using the structural parameters deriving from the structural studies and by assuming that the alloy is a solid solution where the Fe atoms bear the same magnetic moment all through the layers. As in the preceding section, the magnetic moment of Fe is initially assumed to be 2.1 μB. In the case of the Fe-rich SL, the calculation (solid line) fits quite well the experiment in Fig. 3(b). For the Fe 70% SL, it is required to reduce the dichroism signal by a factor 0.13 in

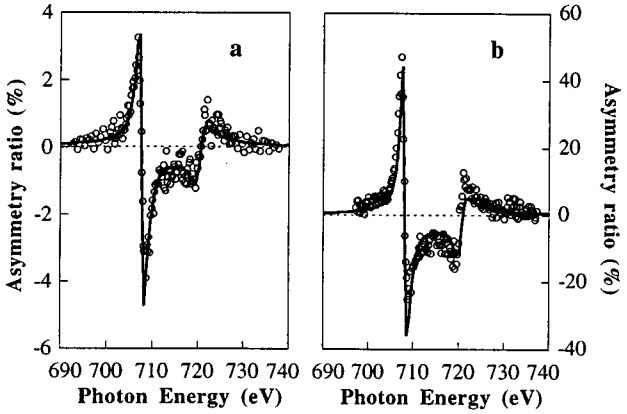

FIG. 3. Energy dependent asymmetry ratio measured at 15° at the Fe $L_{2,3}$ edges on $Fe_{0.7}Mn_{0.3}$/Ir (a) and $Fe_{0.9}Mn_{0.1}$/Ir (b): experiment (open circles) and calculation (solid line).

order to fit the data [Fig. 3(a)]. Therefore, we observe a transition for the Fe magnetic moment from 2.1 ± 0.05 to 0.27 ± 0.05 μB. The uncertainties derive from the dispersion of the fitting parameters of reflectivity curves measured at other angular positions. It is worth recalling that the value for the Fe-rich SL is an averaged one since two phases have been evidenced in the SL. In order to separately determine the magnetic moment in the SL1 phase, we measured the energy dependence of R for the thin $Fe_{0.9}Mn_{0.1}$ films at different angular positions. Using the same set of structural and magnetic parameters, we obtained a good agreement between experiments and calculations. Figure 4(a) shows the asymmetry ratio values obtained at 26° while the ensemble of R measurements will be published in a full article.[15] Again, a fairly good agreement has been obtained with a Fe magnetic moment of 2.1 μB, leading us to conclude that the Fe atoms in SL1 and SL2 carry about the same magnetic moments. Gathering the structural and magnetic informations on the three different phases of the alloy thin films, we observe that the magnetic transition is related neither to the hypothetical fcc or bcc structure of the unstrained layer, nor to the Fe magnetic volume. It actually depends on the c/a value and the transition occurs for $c/a=1.2$[15] which is in agreement with the theoretical prediction for a bct iron.[16]

Work is under progress to understand the magnetic properties of the Mn atoms. Figure 4(b) displays the weak magnetic signal measured at the $L_{2,3}$ edges of Mn in the thin $Fe_{0.9}Mn_{0.1}$ films. It shows that Mn atoms carry a net magnetic moment. We observe the R spectrum has the same shape than that measured at the Fe L edges at the same incident angle. In order to determine the amplitude of the Mn magnetic moment as well as the coupling between Fe and Mn, we have to fit the R values. In the case of Mn, this is not so straightforward, since bulk Mn is antiferromagnetic and shows no circular dichroism. Here, the calculation is performed using the XMCD data from Mn [1 monolayer (ML)]/Fe(001),[17] where the coupling is found to be ferromagnetic and the Mn magnetic moment estimated to be about 1.7 μB.[18] However, to fit the R values, it has been necessary to change the sign of the XMCD data used in the calculation, which implies to consider an AF coupling of Mn moments to the Fe ones. It appears that the amplitude of the XMCD allows us to simulate the amplitude of R and, hence, we estimate the Mn magnetic moment to be about 1.7 μB.

In summary, we have shown that XRMS in *transverse mode* allows to investigate quantitatively the magnetic properties of thin films and multilayers. It turns out that it is possible to analyze small changes in the energy dependent magnetic contribution to the reflectivity. This allows us to measure weak magnetic moment (here 0.2 μB) in a thin buried layer. A refinement procedure applied simultaneously to the angular and energy scans should give more insights about the amplitude of the moments, their distribution inside the layer, and likely about the magnetic roughness at interfaces. Moreover, we show that large magnetic contributions to the reflectivity are available at large angles which should allow developments towards element specific imaging of magnetic domains. This approach could be useful for imaging the behavior of buried magnetic layers.

The authors thank Y. Souche and F. de Bergevin for fruitful discussions on magneto-optic calculations.

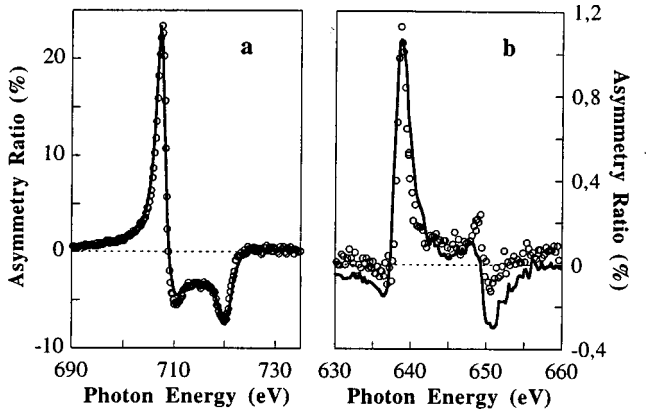

FIG. 4. Energy dependent asymmetry ratio measured on Ir/$Fe_{0.9}Mn_{0.1}$/Ir thin film at 26° at the Fe $L_{2,3}$ edges (a) and at 20° at Mn $L_{2,3}$ edges (b): experiment (open circles) and calculation (solid line).

[1] J. P. Hannon *et al.*, Phys. Rev. Lett. **61**, 1245 (1988); **62**, 2644 (1989).
[2] P. Carra *et al.*, Phys. Rev. Lett. **64**, 1286 (1990).
[3] C. C. Kao *et al.*, Phys. Rev. B **50**, 9599 (1994).
[4] C. C. Kao *et al.*, Phys. Rev. Lett. **65**, 373 (1990).
[5] J. M. Tonnerre *et al.*, Nucl. Instrum. Methods Phys. Res. B **97**, 444 (1995).
[6] J. M. Tonnerre *et al.*, Phys. Rev. Lett. **75**, 740 (1995).
[7] L. Sève, Ph.D. thesis, Univesité Joseph Fourier, 1997 (unpublished).
[8] V. Chakarian *et al.*, J. Magn. Magn. Mater. **165**, 52 (1997).
[9] Y. U. Ydzerda *et al.*, Synchrotron Radiation News **10**, 6 (1997).
[10] B. Vidal and P. Vincent, Appl. Opt. **23**, 1784 (1984).
[11] E. D. Johnson *et al.*, Rev. Sci. Instrum. **63**, 1443 (1992).
[12] C. T. Chen *et al.*, Phys. Rev. Lett. **75**, 152 (1995).
[13] H. Fischer, Ph.D. thesis, Université Nancy, 1995.
[14] A. Déchelette-Barbara *et al.*, J. Magn. Magn. Mater. **165**, 87 (1997).
[15] A. Déchelette-Barbara, Ph.D. thesis, Université Joseph Fourier, 1997 (unpublished).
[16] G. L. Krasko *et al.*, J. Appl. Phys. **67**, 4570 (1990).
[17] S. Andrieu *et al.*, Phys. Rev. B **57**, 1985 (1998).
[18] S. Andrieu *et al.*, Europhys. Lett. **38**, 459 (1997).